THE ASTROPHYSICAL JOURNAL, 275:477–492, 1983 December 15

THE STELLAR AND NONSTELLAR CONTINUA OF SEYFERT GALAXIES: NONTHERMAL EMISSION IN THE NEAR-INFRARED

MATTHEW A. MALKAN AND ALEXEI V. FILIPPENKO
Palomar Observatory, California Institute of Technology
Received 1983 March 24; accepted 1983 May 26

ABSTRACT

Spectra having high resolution and excellent signal-to-noise ratios have been obtained for the nuclei of nine Seyfert galaxies. In Seyfert 1 nuclei the Mg I λ5175, Na I D λ5892, and Ca II λ8542 stellar absorption lines are extremely weak, indicating that galactic starlight does not contribute a significant fraction of the observed continuum. The relative amount of light (in a given aperture) due to the unresolved nucleus of each galaxy has been measured from direct images made with a silicon intensified target (SIT). Knowing the fraction of nuclear light which comes from stars, we deduced the total stellar and nonstellar continuum fluxes in the spectral range λλ5000–8600. Within a 10″ aperture stars contribute a sixth or less of the visual continuum in Mrk 335 and Mrk 509, one-fourth to two-fifths of that in NGC 4151, 5548, and 7469, and three-fifths of that in NGC 1275, 3227, and 4051. These fractions are accurate to 10%–15%. The starlight has colors which are typical of those in the disks of normal spiral galaxies. The nonstellar continuum is similar to that of quasars—it drops from the near-infrared to the visual like a power law with slope $\alpha \sim -1.1$ to -1.2, and in the brighter galaxies it flattens in the blue. Even at minimum brightness, the nonstellar flux has no short-wavelength cutoff near 1 μm, eliminating the possibility that the near-infrared flux is dominated by thermal emission from hot dust grains.

In an appendix, we report several weak emission lines that have not been previously seen in the spectra of active galactic nuclei. Some interesting characteristics of the broad permitted lines, as well as differences in the widths of various forbidden lines, are also mentioned.

Subject headings: galaxies: nuclei — galaxies: Seyfert — galaxies: stellar content — spectrophotometry

I. INTRODUCTION

Nearby Seyfert galaxies have been extensively investigated because they are bright and easy to observe. Their relatively faint nonstellar continuum is more difficult to study, however, because of substantial contamination from starlight. In particular, the spectral shape of the nonstellar continuum has not been unambiguously measured in any low-luminosity Seyfert galaxy; rather, many workers have simply *assumed* that it is similar to that of luminous quasars.

Direct imaging cannot in itself determine the galactic contribution, since much of the starlight may lie within the seeing disk and is inseparable from the pointlike (unresolved) nonstellar light. Nor is low-resolution spectrophotometry of the continuum adequate, as it cannot distinguish a large stellar component with a weak blue nonstellar continuum from a smaller stellar component with a strong red nonstellar continuum (Malkan and Oke 1983). The most effective spectroscopic indicators of a stellar population are prominent absorption lines such as the G band (λ4304), the Mg I *b* triplet (λ5167, λ5173, λ5184), and the Ca II near-infrared triplet (λ8498, λ8542, λ8662). These lines are presumably absent in any nonstellar continuum, and their strengths in normal galaxies are well known. The strong Na I D (λ5890, λ5896) and Ca II H (λ3968) and K (λ3934) lines can also be useful, but they may be contaminated by interstellar absorption in the host galaxy (Osterbrock 1978, 1983).

Osterbrock (1978, 1983) gave estimates or upper limits to the starlight components of many Seyfert 1 spectra from the strength of the Ca II K line. However, the slit size was small (2″.7 × 4″.0), so these measurements refer only to the nucleus. Direct imaging is required to estimate the starlight contribution seen in large apertures. In addition, the nonstellar light in Seyfert 1 galaxies is much bluer than that of stars, and it is therefore essential to measure the stellar flux at longer wavelengths, where its relative strength is greater. Finally, since the nonstellar continuum often varies by more than a magnitude on time scales of a month (Penston *et al.* 1974), images and spectra should be obtained contemporaneously. Malkan and Oke (1983) used this combination of slit spectroscopy and direct imaging of the Seyfert galaxies Mrk 3, Mrk 6, and NGC 1068. Their spectra

had reasonably good signal-to-noise ratios, but only 7 Å resolution, and it is not easy to separate weak absorption lines from adjacent emission lines.

In this paper, digital images of nine Seyfert galaxies are combined with coudé spectra having excellent signal-to-noise ratios and high resolution in order to more precisely estimate the stellar flux and to determine the nature of the remaining continuum. The observations are presented in § II, and the methods used to analyze them are outlined in § III. Section IV discusses the host galaxies, whereas § V examines properties of the nonstellar continuum. A brief summary of our main conclusions is given in § VI.

II. OBSERVATIONS

Direct images were obtained with the SIT Area Photometer (Kent 1979) on the Palomar 1.5 m telescope, as listed in Table 1. The data come in the form of a 256×256 array of square pixels, each 0.″7 on a side, giving a $3' \times 3'$ field of view. To maximize the dynamic range, the photocathode was run at a relatively low gain, corresponding to a saturation level of 10,000 photons per pixel. The required integration times for our bright objects were still only 10–600 s, and two or three consecutive exposures of each galaxy were usually taken. The light passed through square filters selected to exclude significant contamination from emission lines. Most images were obtained through either a Gunn violet (v) filter (Thuan and Gunn 1976), with $\lambda_0 = 4000$ Å and $\Delta\lambda = 400$ Å, or a Wratten 88A filter, which gives $\lambda_0 = 7900$ Å, $\Delta\lambda = 1200$ Å, corresponding approximately to the i magnitude defined by Wade *et al.* (1980). A few images were obtained through narrow-band ($\Delta\lambda = 100$ Å) filters centered on either 6615 Å or 6760 Å, which were kindly loaned by Dr. H. C. Arp. For each galaxy, the filter was selected to avoid the strong Hα + [N II] emission lines; thus the 6760 Å filter was used for low-redshift galaxies, and the 6615 Å filter for objects of higher redshift. Comparison with the absolute spectrophotometric scans of de Bruyn and Sargent (1978) shows that contamination from line emission in all these filters was negligible.

An average zero-level picture was removed from each frame, and pixel-to-pixel sensitivity variations were eliminated by flattening with a lengthy exposure of the illuminated dome ceiling. The sky measured in a large (typically $\gtrsim 1'$) annulus centered on the galaxy was subtracted from each exposure. Since this correction was well determined, and generally less than 10% of the central brightness of the galaxy, it is a small source of uncertainty in the derived surface brightness profiles. The photometric zero points were set by several measurements of defocused standard stars and are accurate to 10%. Spatial distortions in the SIT frames were negligible in the regions of interest.

Spectra having ~ 1.6 Å resolution were obtained with a photon-counting Varo-Reticon detector (Shectman and Hiltner 1976) at the coudé focus of the Mount Wilson 2.5 m Hooker telescope. A small aperture ($\sim 1.''6 \times 3.''7$) isolated light from the nuclear seeing disk. An image

TABLE 1

JOURNAL OF OBSERVATIONS (UT)

Galaxy	Coudé Spectroscopy	Direct Imaging	Optical Spectrophotometry	Infrared Photometry
NGC 1068 ...	1982 Jan 4 (Mg)	1981 Oct 16	...	...
	1982 Nov 14 (Na)	1982 Mar 7	...	...
	1981 Oct 24 (Ca)	...	...	...
NGC 1275 ...	1981 Oct 22,23 (Mg)	1981 Oct 9,10,14,16	...	...
NGC 3227 ...	1981 Mar 29 (Mg)	1981 Apr 1	...	...
	1982 Nov 14,15 (Mg)	...	...	...
	1981 Jan 10 (Na)	...	...	...
NGC 4051 ...	1981 Mar 28 (Mg)	1981 Apr 1	1979 Jun 12	1978 Feb 22
	1982 May 22 (Mg)	1982 May 20	...	1980 Mar 25
	1982 Apr 19 (Na)	...	...	1980 Mar 30
	1982 May 21 (Na)	...	...	...
NGC 4151 ...	1981 Mar 29 (Mg)	1981 Apr 1	1980 Mar 9	1980 Feb 11
	1982 May 22 (Mg)	1982 Mar 7	1979 Apr 16	1980 Mar 30
	1982 Apr 19 (Na)	1982 May 20	...	1979 Apr 13
	1982 Apr 20 (Ca)	...	...	1979 May 6
NGC 5548 ...	1981 Mar 30 (Mg)	1981 Apr 1	1980 Mar 9	1980 Mar 30
	1982 May 22 (Mg)	1982 Mar 7	...	1980 Apr 15
	1982 May 21 (Na)	1982 May 21	...	...
NGC 7469 ...	1981 Oct 22 (Mg)	1981 Aug 9	1980 Sep 30	1980 Oct 25
	1982 Nov 14 (Na)	1981 Oct 10,15,17	1979 Jun 12	1979 Jun 29
Mrk 335	1981 Oct 23 (Mg)	1981 Aug 9	...	...
	1982 Nov 15,16 (Na)	1981 Oct 10,15,16	...	...
Mrk 509	1982 May 21 (Na)	1981 Aug 9, Oct 14,16	...	...

derotator was not used because of the unacceptably large light losses it would have caused. The sky was measured in an identical aperture displaced by ~ 6″, and appropriate corrections were applied when light from the galactic disk contaminated the sky spectrum. Owing to the very steep surface brightness profiles in Seyfert galaxies, these corrections were generally very small, but in several cases (e.g., NGC 1068) we obtained additional sky spectra a few arc minutes away from the object to achieve greater accuracy. Standard stars (Oke and Gunn 1983) were used to calibrate the instrumental response, and all observations were divided by the spectrum of an intrinsically featureless continuum from a tungsten lamp to remove local variations in the detector sensitivity. Wavelengths were calculated from Fe–Ar arcs taken several times throughout the night. There were gradual drifts in the wavelength scale, but the calibration should be accurate to ~ 0.3 Å. Atmospheric absorption lines were removed by comparison with the spectra of early B stars.

III. ANALYSIS

a) Direct Images

The radial surface brightness profiles for each object were derived by azimuthally averaging the signal as a function of distance from the image center. Repeated measurements on different nights show that these curves are accurate to 0.1 mag for radii up to 15″. The same information is also available as the integrated fluxes within a series of concentric circles centered on the peak brightness of the galaxy. A typical example of these two forms (differential and integral) of displaying the data is shown for NGC 5548 in Figures 1 and 2. The following analysis does not assume the galaxies are azimuthally symmetric: we simply refer all measurements to circular apertures for convenient comparison with other observations.

The galaxy profiles were then compared with those of field stars on the same frames to determine the resolved fraction of galaxy light. That is, a stellar (unresolved) seeing profile was scaled to match the galaxy profile in the central few arc seconds. Any remaining galaxy light above this profile is resolved and presumed to arise from stars, as shown in Figures 1 and 2. The scaled seeing profiles match the inner parts of the galaxy profiles with high precision: the residuals are only 2%–3%, smaller than the width of the lines in Figure 1.

The limiting source of error in this procedure was the accuracy with which the seeing profile could be determined at the time each Seyfert nucleus was measured. When a single frame had more than one bright stellar image, their surface brightness profiles were always very similar, with full widths at half-maximum (FWHM) ~1.″4–1.″9. On average, the seeing profile was independent of wavelength. However, there were small but

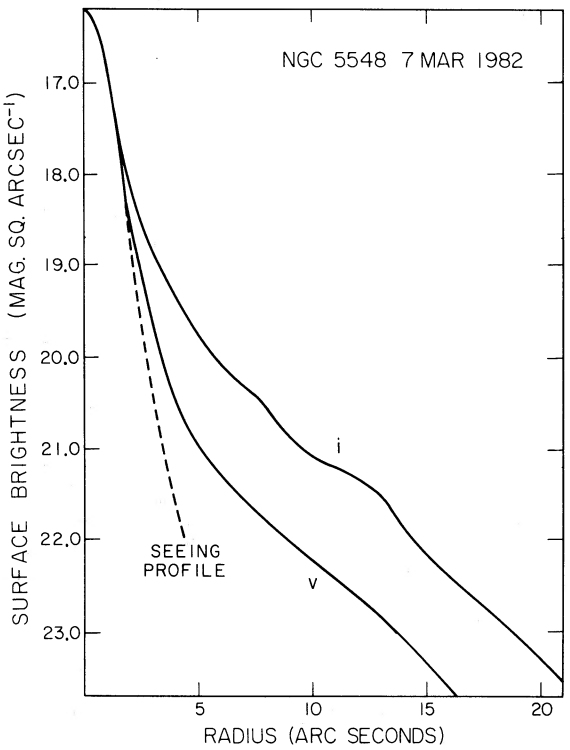

FIG. 1.—Surface brightness profiles of NGC 5548, observed through *v* and *i* filters. The violet and infrared fluxes are comparable in the predominantly nonstellar nucleus. At larger radii, the infrared/violet flux ratio increases, leveling off at the much redder color typical of a galaxy. The dashed line is a seeing profile, scaled to match the center of the *i* brightness distribution in NGC 5548. In other words, it shows the portion of light in NGC 5548 which is unresolved.

detectable changes in the profile of a single star observed in two consecutive exposures, and gradual changes in the seeing occurred throughout the course of a night. Roughly half of the program galaxies did not have a bright field star in the same frame, so we compared these with stellar images observed either immediately before or after the galaxy. Owing to the seeing fluctuations, our estimates of the unresolved fractions are only accurate to 10%–15%. That is, two stellar images obtained in the same part of a night were often not identical. Compared with the sharper image, the poorer one had up to 10%–15% of its light "resolved." This dominant source of error was reduced by averaging the results of several frames. Possible errors in the photometric zero points would not alter the *fractions* of resolved light we found by this procedure.

Our estimates of the fraction of resolved light in NGC 5548 and NGC 7469 agree with those obtained by de Bruyn (1982) in 1978 June. In several cases, galaxies were imaged on more than one night. Even when their nuclear brightness varied, we found the same amount of starlight present, to within 0.10–0.20 mag. This is a

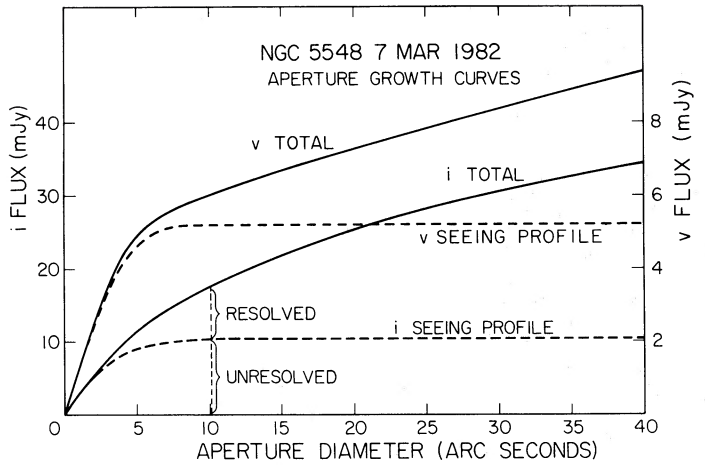

FIG. 2.—The integrated flux as a function of diameter enclosed by a circular aperture centered on the nucleus of NGC 5548. The scale for the violet fluxes is on the right; the infrared fluxes are plotted on a scale which is a factor of 5 larger. The dashed lines show seeing profiles (derived from images of field stars) normalized to match the galaxy growth curves at the smallest diameters. They correspond to the fraction of the light which is unresolved: 5.4 mJy at 4000 Å and 10.8 mJy at 7900 Å. The sharp bend in the v curve indicates that the nucleus of NGC 5548 dominates at 4000 Å; the image at 7900 Å is more extended because the starlight is much redder than the light from the nucleus.

reasonable measure of the total uncertainties associated with the estimates of starlight fluxes, which are listed in Table 2. The errors for NGC 3227 are somewhat larger since it was imaged on only one night.

b) Spectra

The unresolved continuum comes from the pointlike nonstellar nucleus and the starlight of the central part of the galaxy which falls within the seeing disk. Our spectra were used to estimate the ratio of unresolved stellar to nonstellar flux, under the assumption that the fraction of light in the nucleus due to stars is simply the ratio of the observed equivalent width of a stellar absorption line to its average value in the spectrum of an ordinary galaxy.

Figures 3–5 illustrate all of the spectra included in our analysis, with the exception of some repeat observations. The relative flux per unit frequency interval is plotted as a function of wavelength, and both scales are linear. Wavelengths have been reduced to the rest system of the observed galaxy. Since small apertures and long integration times were used, in some cases atmospheric dispersion produced substantially unequal light losses in different portions of a spectrum (Filippenko 1982). Therefore, to flatten the continuum for accurate measurements of absorption lines, every spectrum was normalized by fitting a cubic spline through the continuum and dividing the flux in each bin by the local value of the spline. This technique artificially removes any broad intrinsic spectral shape, so the true relative intensities of regions separated by more than ~100 Å

TABLE 2

FLUXES AT 5400 Å (mJy)

	WITHIN 10″ APERTURE		TOTAL STARLIGHT WITHIN APERTURE OF:			
GALAXY	Stellar	Nonstellar[a]	15″	20″	25″	30″
NGC 1068 ...	65	17	100	140	180	220
NGC 1275 ...	5.2	2.9	9.3	13	15	17
NGC 3227 ...	7.6	5.2	14	19	25	...
NGC 4051 ...	7.3	5.7	10	13	16	19
NGC 4151 ...	14	21/29[b]	21	28	34	40
NGC 5548 ...	3.4	6.9	5.6	7.4	9.0	10
NGC 7469 ...	6.8	7.5/12[b]	7.9	10	13	15
Mrk 335.....	1.5	7.4	...	...	...	...
Mrk 509.....	1.5	8.6	...	...	...	...

[a]The nonstellar flux (f_ν) is approximately a power law with slope −1.1 to −1.2 in all cases.

[b]The two nonstellar fluxes refer to measurements when the continuum was faint and when it was bright.

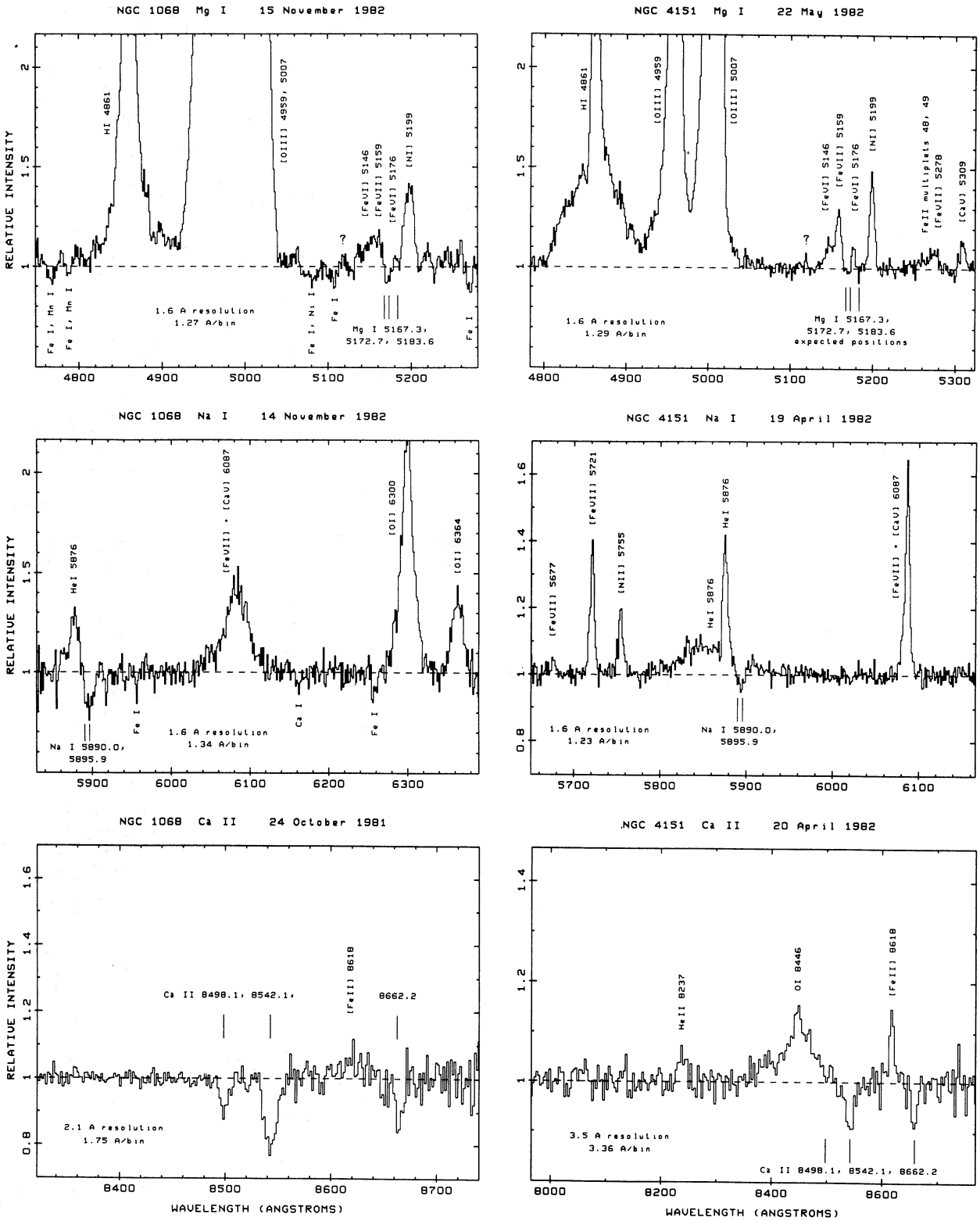

FIG. 3.—Coudé spectra, shifted to zero redshift, of NGC 1068 and NGC 4151 near the Mg *b*, Na D, and Ca II near-infrared absorption lines. The continuum has been normalized to unity in each case, and relative intensities refer to flux per unit frequency interval. Very low and high flux levels are not plotted in order to emphasize the continuum. The emission feature indicated by a question mark is an unidentified line at $\lambda \sim 5120$ Å.

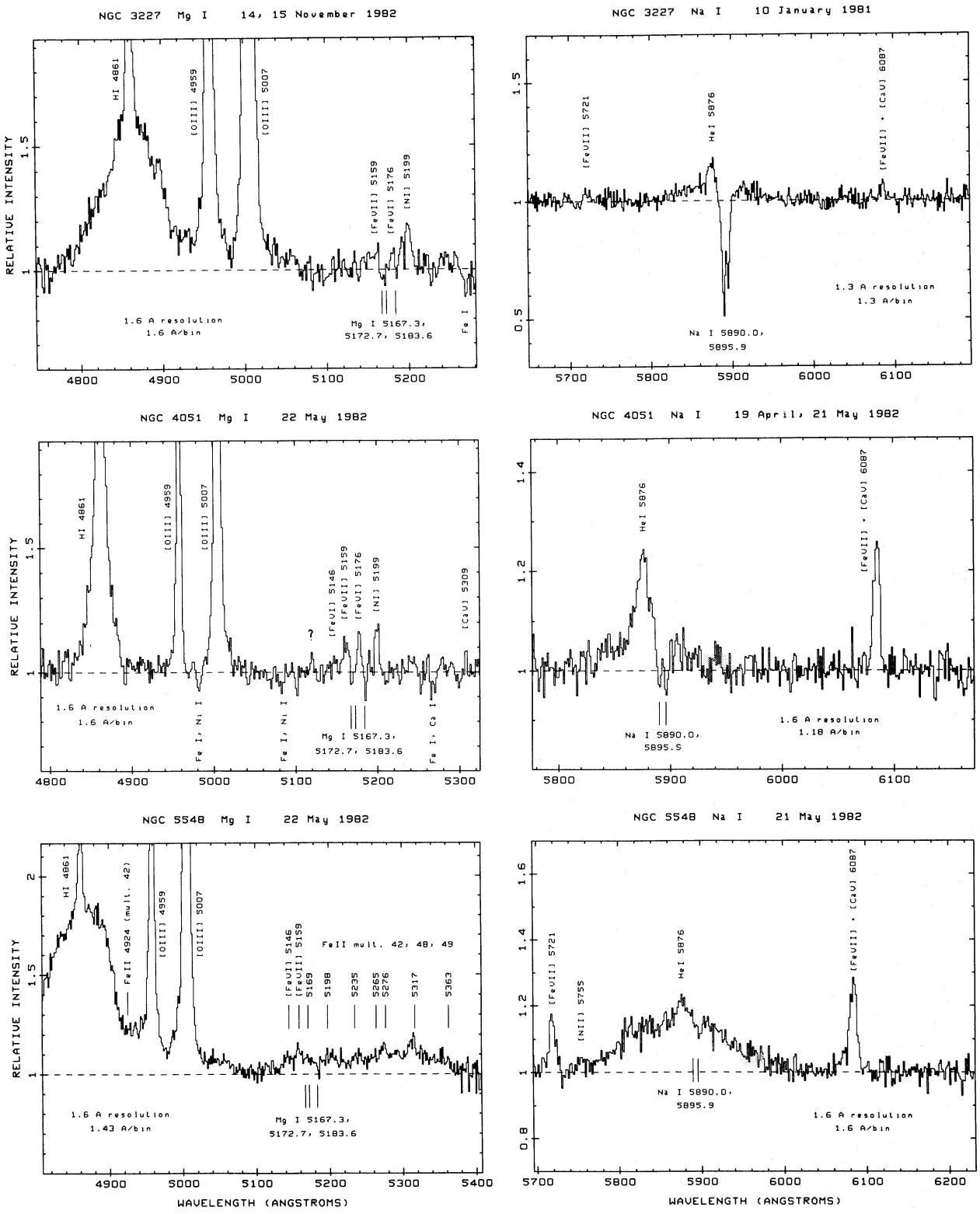

FIG. 4.—Same as Fig. 3, but for NGC 3227, 4051, and 5548 near Mg *b* and Na D

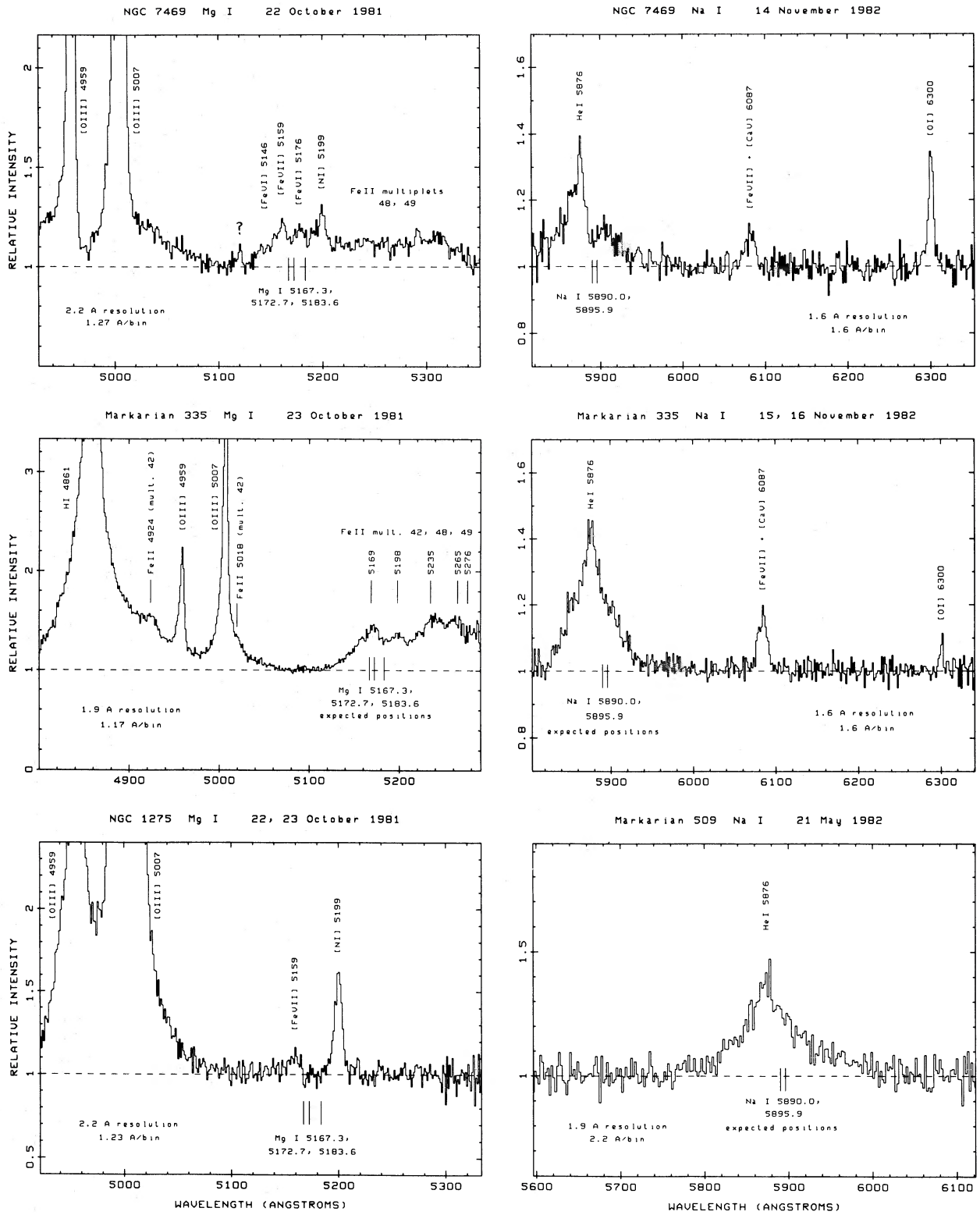

FIG. 5.—Same as Fig. 3, but for NGC 1275, NGC 7469, and Mrk 335 near Mg *b*, and for NGC 7469, Mrk 335, and Mrk 509 near Na D

are not displayed exactly. Note that in most spectra the relative scale is adjusted to emphasize the continuum, so very low or high flux levels are not plotted.

Although they are potentially useful indicators of starlight, the G band and the Ca II H and K lines were not observed because of the increasing proportion of nonstellar light and, in particular, the decreasing detector sensitivity at short wavelengths. Similarly, the Ca II near-infrared triplet could be measured in only the brightest nearby galaxies NGC 1068 and NGC 4151, as the efficiency of the system plummets longward of ~ 8000 Å.

Prominent emission and absorption lines (or the expected position of absorption lines) are marked on the spectra. The equivalent widths of absorption features were measured in the standard manner, but some difficulties were encountered with Mg *b* and Na D. For example, galaxies such as NGC 1068, 3227, 4051 and 4151 exhibit strong forbidden lines of nitrogen and highly ionized iron which contaminate the Mg *b* absorption, as well as narrow He I λ5876 near the Na D doublet. These emission lines could be removed to first order because the high spectral resolution adequately isolated them from the absorption lines. Permitted lines of Fe II presented an additional problem near Mg *b*, as can be seen in Mrk 335, NGC 5548, and NGC 7469. The spectra were compared with those published by Phillips (1977, 1978), and once again our high spectral resolution was necessary for accurate measurement of the absorption lines. Finally, a suitable correction was made to the equivalent width of Na D in objects which show broad He I λ5876 emission, and in spectra from which broad Na D emission (due to high-pressure sodium vapor lamps) could not be completely subtracted.

Our assumption that the spectra measure only unresolved nuclear light is conservative, since light from the galactic disk entered near the ends of the long (3″.7) aperture. Furthermore, if some off-nuclear light entered the aperture because of guiding errors or atmospheric dispersion, the strengths of absorption lines would be overestimated. Despite these effects, the absorption lines in most of the spectra are extremely weak, indicating that the unresolved light is almost entirely nonstellar.

Since some Na D absorption may arise from the interstellar medium of the host galaxy, the true equivalent width of the stellar absorption could be even smaller than the values listed in Table 3. NGC 3227 has extremely strong, narrow Na D absorption (Fig. 4), which seems inconsistent with its very weak Mg *b* lines. NGC 4051 also exhibits an easily resolved Na D doublet, in contrast to the stellar Na D absorption in the bulge of NGC 1068 (Fig. 3). The nucleus of NGC 3227 is obscured by $A_V \sim 1.4$ mag, and NGC 4051 could have half as much extinction (Malkan 1983*a*). We suspect that most of the Na D absorption in these two objects (and possibly in others as well) is interstellar. Na D absorption due to our Galaxy did not present any difficulties, since $cz \gtrsim 1000$ km s^{-1} for all of the Seyfert galaxies observed.

The equivalent widths of stellar absorption lines in the spectra of Seyfert nuclei are given in Table 3. Our measurements may be somewhat generous: the true widths could be less, but they certainly do not exceed the ones listed by more than ~ 25%, so it is unlikely that the contribution due to stars has been significantly underestimated. Since the absorption lines are very weak in most of the objects, we were concerned primarily with the danger of underestimating the starlight contribution; such an error would have an important impact on our conclusions. The small equivalent widths listed for the Mg *b* lines are in good agreement with the Ca K widths measured by Osterbrock (1978) in these objects

TABLE 3

COUDÉ SPECTROSCOPY: EQUIVALENT WIDTHS (Å)

Galaxy	Mg I *b*	Na I D	Ca II λ8542[a]
Average spiral[b] ...	4.5 ± 2.1	3.7 ± 1.6	3.2 ± 0.5
NGC 1068	1.7	2.9	3.0
NGC 1275	0.25	...	...
NGC 3227	0.75	4.2	...
NGC 4051	0.8	1.1	...
NGC 4151	0.2	0.8	1.1
NGC 5548	0.2	0.3	...
NGC 7469	0.3	0.7	...
Mrk 335.....	< 0.1	< 0.2	...
Mrk 509.....	...	< 0.25	...

NOTE:—The symbol < means line not detected or only marginally detected—upper limit given.

[a] Ca II refers to the width of one component of the triplet, at 8542 Å; the other two lines (8498, 8662 Å) were more difficult to measure.

[b] Average spiral: Mg *b* and Na D from Hartwick and Cowley 1980 and Stauffer 1983. Ca II from Cohen 1978.

c) *Stellar and Nonstellar Fluxes*

In order to determine the amount by which galactic absorption lines have been diluted by a nonstellar featureless continuum, we must know the intrinsic strengths of the lines. The spectra measured light from roughly the central kiloparsec of each object, where the bulge dominates the contribution from the disk component in early- and intermediate-type spiral galaxies. Since the integrated spectra of galactic bulges are dominated by red giants, the strengths of stellar absorption lines do not vary greatly from galaxy to galaxy. Cohen (1978) found that the near-infrared Ca II triplet lines have relatively constant equivalent widths in different galaxies and exhibit no spatial variations in a given object. The equivalent widths of Mg *b* and Na D in Table 3, taken from Hartwick and Cowley (1980) and Stauffer (1983), are averages over all types of spiral galaxies. The larger variations seen in the *b* and D lines are due to metallicity differences and dilution from the blue continuum of hot young stars.

Although these variations in equivalent width are a nonnegligible source of error in our analysis, it is likely that the stellar population in the nuclei of Seyfert galaxies more closely resembles that of elliptical or early-type spiral galaxies than that of late-type spirals. Thus, the *effective* scatter in the width of a line is probably smaller than indicated in Table 3. For example, late-type spiral galaxies exhibit relatively weak Mg *b* absorption, but their stellar population is probably not representative of Seyfert 1 nuclei since features such as Fe I λ5269, whose strengths should be comparable to that of Mg *b* (Osterbrock 1983), are not visible (except weakly in NGC 1068 and NGC 3227).

The direct imaging gives R, the ratio of resolved to total light within a 10″ aperture (as illustrated in Fig. 2). To compare estimates made at different wavelengths, we assume that the starlight spectrum is that of the "standard galaxy" of Yee and Oke (1978), in which the ratios of flux at 4000, 5200, 6600, and 8000 Å are 0.33 : 1.0 : 1.5 : 2.3. As illustrated by Malkan and Oke (1983), it is a good match to the integrated spectra of early-type galaxies and to the central regions of later-type spiral galaxies, which are dominated by bulge light from red giants.

The starlight flux at 5200 A in a 10″ aperture is given by

$$F_*(5200) = C_*(\lambda)\,F(\lambda)\left[R + (1-R)(\mathrm{EW}_{\mathrm{obs}}/\mathrm{EW}_*)\right],$$

where the measurements of *total* flux $F(\lambda)$, R, and absorption equivalent width ($\mathrm{EW}_{\mathrm{obs}}$) are made at a wavelength λ. The quantity $C_*(\lambda)$ is the standard galaxy color $F_*(5200)/F_*(\lambda)$, and EW_* is the equivalent width of the absorption line in the case of pure starlight. The first term, $C_*(\lambda)F(\lambda)R$, is the resolved (extended) flux, which is, by assumption, entirely stellar. The second term is the portion of the unresolved nucleus which is starlight, as manifested by absorption lines in our spectra. In all objects the first term is larger than the second, since ($\mathrm{EW}_{\mathrm{obs}}/\mathrm{EW}_*$) is typically 0.05–0.20 and tends to be smallest when R is small (e.g., in Mrk 335 and Mrk 509).

Errors in the photometric zero points [leading to incorrect $F(\lambda)$] and those in the galaxy color $C_*(\lambda)$ propagate linearly as errors in the estimated stellar flux. We confirm in § IV that the galaxy colors are indeed very similar to those of our standard galaxy, so the second source of error is negligible. For the values listed in Tables 2 and 3, it is evident that the dominant source of error comes from 10%–15% uncertainties in R, although the second term tends to offset errors in the first. As long as a portion of the seeing disk is contaminated by starlight (i.e., as long as $\mathrm{EW}_{\mathrm{obs}}/\mathrm{EW}_*$ exceeds zero), the resolved flux ratio (R) tends to increase as the seeing improves, but this improvement in the seeing also decreases $\mathrm{EW}_{\mathrm{obs}}/\mathrm{EW}_*$. If the seeing is *identical* during the direct and spectroscopic observations, its effects cancel. On the other hand, if it is much *worse* during the direct observations, the starlight flux is underestimated. It is probable that any differences in our observations were actually in the opposite sense: the direct images were generally obtained under slightly better seeing conditions than the spectra (if we include guiding errors in the effective "seeing"). In the next section we confirm that seeing did *not* lead to an underestimate of the stellar flux.

The additional photometric errors and uncertainties in EW_* lead to estimates of stellar and nonstellar flux in Table 2 that are accurate to 15%–20%. Aperture growth curves were used to calculate the total amount of visual continuum flux from stars in 10″–30″ apertures (Table 2).

IV. THE HOST GALAXIES

Having separated the stellar and nonstellar continuum in each Seyfert nucleus, we can now compare the host galaxies with others which lack active nuclei. As Yee (1983) concluded for 11 Seyfert 1 galaxies, the nuclear colors (dominated by nonstellar light) are much bluer than those of starlight. But it is relatively easy to measure the colors at radii larger than 5″, where contamination from the unresolved nucleus is negligible. The starlight colors measured 5″–30″ from the nuclei of NGC 4051, 4151, 5548, and Mrk 335 are approximately the same as those of the standard galaxy. Colors were not measured in NGC 3227 and Mrk 509.

The type 2 Seyfert galaxy in our sample, NGC 1068, shows little color change from the nucleus to a radius of ~ 7″. At larger radii (8″–17″), the color becomes bluer than that of a standard galaxy by 0.2 mag in $v - r$. This is due to the contribution from bright rings of H II regions and their associated young stars, which are

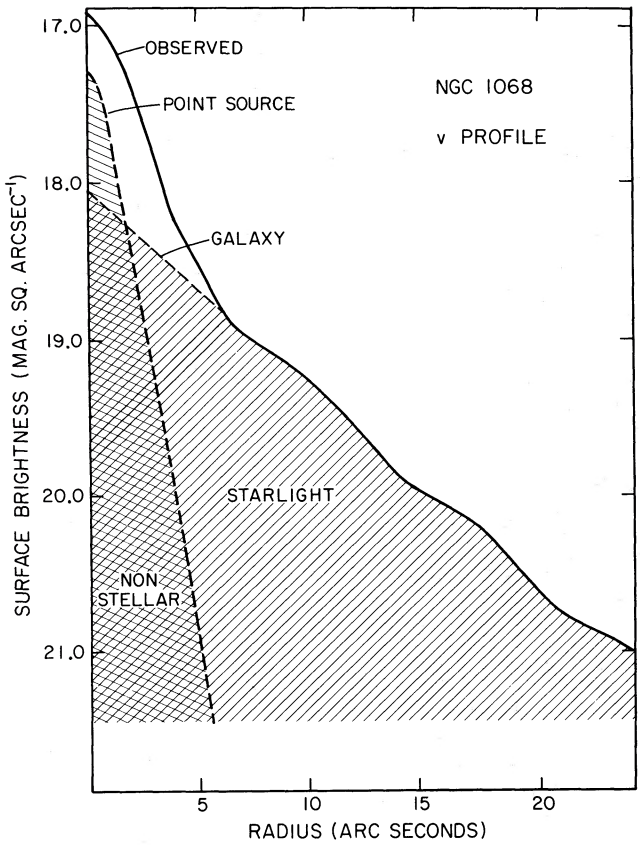

FIG. 6.—The observed violet surface brightness profile of NGC 1068, and its decomposition into an unresolved nonstellar component (*hatched region bounded by the dashed line labeled "point source"*) and a galactic starlight component (*hatched region bounded by the dashed line labeled "galaxy"*). The sum of the nonstellar and stellar components is equal to the observed profile (*solid line*). Integrating the galaxy curve and assuming a normal starlight color yields the stellar flux estimates given in Table 2. At the nucleus ($r \sim 0$) stars make up about a third of the light at v, in excellent agreement with the spectroscopic results.

evident on photographs having short exposure times (Alloin *et al.* 1981). The FWHM of the Na D and Ca II near-infrared lines is 470 ± 40 km s^{-1}, and the corresponding velocity dispersion (200 ± 20 km s^{-1}) is at the high end of observed values in bulges of spiral galaxies (cf. Kormendy and Illingworth 1982).

We checked our estimates of the stellar flux *in the nucleus* at several different wavelengths to see if they are consistent with the light from a standard galaxy. In all cases except NGC 1275, the inferred galaxy colors are the same as those of the standard galaxy to within 0.1–0.2 mag. NGC 1275 is unusual in that $v - g$ does not change by more than 5% from the nucleus out to a radius of 15″. Thus, its nucleus and the nearby starlight both have roughly the same blue color, $v - g \sim 0.25$, which is several tenths of a magnitude bluer than the standard galaxy. The additional blue light around the nucleus of NGC 1275 probably comes from a population of young stars, as has already been revealed by previous observations of Balmer absorption lines in off-nuclear spectra (Minkowski 1968).

We agree with Yee (1983) that the starlight in most Seyfert galaxies has the colors of typical spiral disks. That is, it is only slightly bluer than an elliptical galaxy. Malkan, Margon, and Chanan (1983) found the same result from imaging quasars of low redshift selected from X-ray surveys.

The surface brightness profiles allow one critical check for consistency with the spectroscopy. As illustrated in Figures 6 and 7 for NGC 1068 and NGC 4151, we can use the images to estimate the total stellar flux by a method which is completely independent of the spectroscopy. Guided by the portion of the profile outside $r = 3''$, which is entirely starlight, we smoothly extrapolate (as indicated by the thin dashed line) the galaxy flux to $r = 0''$, much as Yee (1983) did in his analysis. We then compare the inferred central surface brightness of the stars with the observed central surface brightness to find what fraction of the nuclear light is stellar. Approximately a third of the v light in the nucleus of NGC 1068 is predicted to be stellar, and in NGC 4151 stars should contribute a tenth of the v light and a third of the

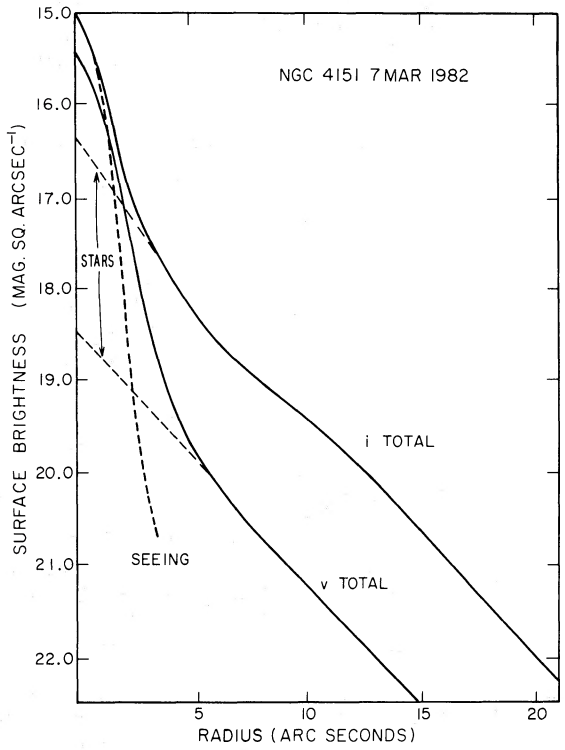

FIG. 7.—The observed v and i surface brightness profiles of NGC 4151. The starlight component is shown extrapolated into the nucleus by the thin dashed lines. The i seeing profile is shown by the heavy dashed line.

i light. These predictions are in excellent agreement with the observed absorption-line strengths, confirming our assumptions that the seeing was similar during the direct and spectroscopic observations, and that the intrinsic strengths of absorption lines in the stars were normal.

V. THE NONSTELLAR CONTINUUM

The estimates of starlight flux in the preceding section allow us to isolate the spectra of the nonstellar continuum. Several of the galaxies in this program have been observed nearly simultaneously at infrared and optical wavelengths. The observing dates are given in Table 1. Optical spectrophotometry was obtained through a 10″ aperture by de Bruyn, Sargent, and Readhead (1982) with the multichannel spectrometer (Oke 1969) on the Hale 5 m telescope. Near-infrared photometry (1.2–3.5 μm) was obtained with the Las Campanas du Pont 2.5 m and Mount Wilson 1.5 m reflectors, or taken from previous studies by Rieke (1978), McAlary *et al.* (1983), Cutri *et al.* (1981), Rudy *et al.* (1982), McAlary, McLaren, and Crabtree (1979), and Balzano and Weedman (1981). Our new infrared photometry is presented in Table 4. Most of the measurements were made with 8″–12″ apertures, so that only very minor corrections were required before combining the infrared with the optical observations, as has been done in Fig. 8. The data are plotted as vertical bars. We also include measurements made at 10 μm, although generally these were not simultaneous with the other observations. If there is significant variability at 10 μm in any of these galaxies, this portion of the composite spectra should be considered more uncertain.

In Mrk 335 and Mrk 509, the correction for starlight included in a 10″ aperture is 15% or less and can almost be ignored completely. The corrected nonstellar continua look very similar to the multichannel spectra published by de Bruyn and Sargent (1978). However, starlight comprises a significant fraction of the light within 5″ of the nucleus in all of the other Seyfert galaxies. Figure 8 shows the infrared and optical spectra of NGC 4051, 4151, 5548, and 7469 obtained through a 10″ aperture. Channels containing strong emission lines were excised. The dashed line shows the estimated flux due to stars (from Table 2), and the solid line is the remaining nonstellar light (which is the difference between the bars and the dashed line). Although optical and infrared photometry is available for NGC 1275, we did not attempt a subtraction because, as discussed above, we suspect its starlight is bluer than that of the standard galaxy. For two galaxies, NGC 4151 and NGC 7469, combined infrared and optical data are available

TABLE 4

NEW INFRARED MAGNITUDES

Galaxy	J(1.2 μm)	H(1.6 μm)	K(2.2 μm)	L(3.5 μm)	N(10.6 μm)	Aper.	Date	Tel.[a]
NGC 1068	...	...	...	...	0.96±0.16	9	1979 Sep 6	M60
NGC 1275	...	...	9.83±0.08	...	4.14±0.24	12/9[b]	1979 Sep 7	M60
NGC 7469	...	...	9.14±0.08	...	4.12±0.19	12/9[b]	1979 Sep 6	M60
	10.97±0.03	10.08±0.03	9.34±0.03	8.25±0.05	...	11	1980 Jun 29	L100
	10.54±0.03	9.80±0.03	9.14±0.03	8.00±0.05	...	18	1980 Jun 29	L100
	10.35±0.03	9.57±0.03	9.00±0.03	...	...	63	1980 Aug 1	C36
Mrk 335	...	...	...	...	5.47±0.21	9	1979 Sep 7	M60
Mrk 509	11.99±0.03	11.14±0.03	10.18±0.03	8.70±0.05	...	10	1980 Jul 3	L100

[a]M = Mount Wilson, L = Las Campanas, C = Cerro Tololo. Numbers refer to telescope mirror diameter (inches).
[b]Larger aperture refers to measurement at shorter wavelength.

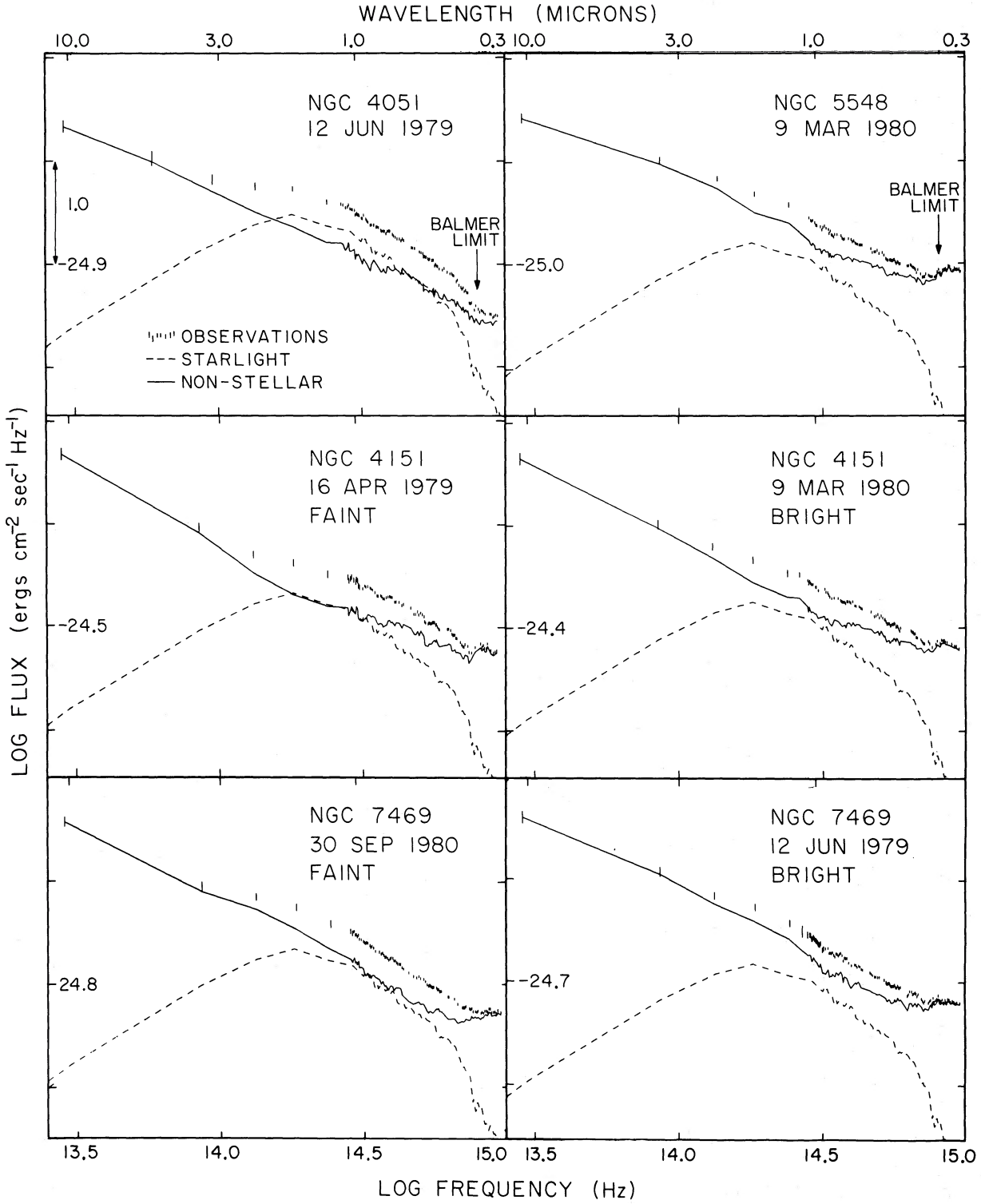

FIG. 8.—Decomposition of the spectra of NGC 4051, 4151, 5548, and 7469 at optical and infrared wavelengths. Bars represent the total observed fluxes in a 10″ aperture. The dashed line shows the amount of flux due to starlight, as given in Table 2, and the solid line is the remaining nonstellar flux found by subtracting the dashed line from the observed fluxes. Arrows indicate the frequency of the Balmer limit. All objects have a marked contribution from blended Balmer lines and continuum which reaches its maximum value at 3650 Å. The spectra on the left side have low-luminosity nonstellar components, which resemble a power law of slope −1.2, but with slight downward curvature. Those on the right have brighter nonstellar components which are more similar to the spectrum of Mrk 509.

for two epochs—one in which the nuclei were near their maximum brightness, and one when they were near minimum. NGC 4051 has never shown optical variations greater than ~ 0.3 mag.

All of the nonstellar spectra exhibit a decrease in slope near 4000 Å ($\log \nu = 14.875$) and then level off at ~ 3650 Å ($\log \nu = 14.915$). Malkan and Sargent (1982; hereafter MS) have already seen this feature in six Seyfert galaxies. The exact wavelength coincidence lead them to attribute it to blended Balmer lines and strong emission in the Balmer continuum. Our results strengthen their view that it is always present in the spectra of Seyfert galaxies.

In Figure 9 we have shifted the nonstellar spectra on top of each other, in two distinct groups. The "faint" group includes NGC 4151 and NGC 7469 near minimum, and NGC 4051. These spectra are slightly steeper and show no indication of any flattening before the Balmer jump which could be attributed to thermal emission (MS). The "bright" group includes NGC 4151 and NGC 7469 near maximum, and NGC 5548. Their nonstellar spectra are almost identical to the spectrum of Mrk 509, which is plotted for comparison. They show a small but significant flattening in the visual, considerably *before* the blending of Balmer lines merges into the Balmer continuum. This characteristic "ultraviolet excess" (or "blue bump") is present in nearly all luminous Seyfert 1 galaxies and quasars. It has been analyzed in detail by MS and by Malkan (1983*b*), who found that it is best interpreted as thermal emission from optically thick accreting gas. The two least luminous Seyfert galaxies studied by MS were NGC 4151 and NGC 5548, for which only an upper limit on the strength of the thermal ultraviolet emission could be established. The present measurements of starlight in NGC 4151 and NGC 5548 provide a more precise estimate of their nonstellar spectra, and it is now evident that when they are bright, they also flatten around 5500 Å (Fig. 9). Thus, the less luminous Seyfert nuclei can show the same signature of optically thick thermal ultraviolet emission that MS concluded was present in all brighter objects.

All the nonstellar spectra slope down from 10 μm to the visual roughly like power laws ($f_\nu \propto \nu^\alpha$) with slopes (α) of -1.1 to -1.2. This characteristic shape is commonly seen in most broad emission-line objects, as discussed by MS. A closer look reveals that the spectra are not exactly described by power laws but usually have a slight downward curvature, as mentioned by Malkan (1983*b*) and others. The logarithmic slope from 0.8 to 2.5 μm is one- or two-tenths steeper than the slope from 2.5 to 10 μm. It seems reasonable to expect

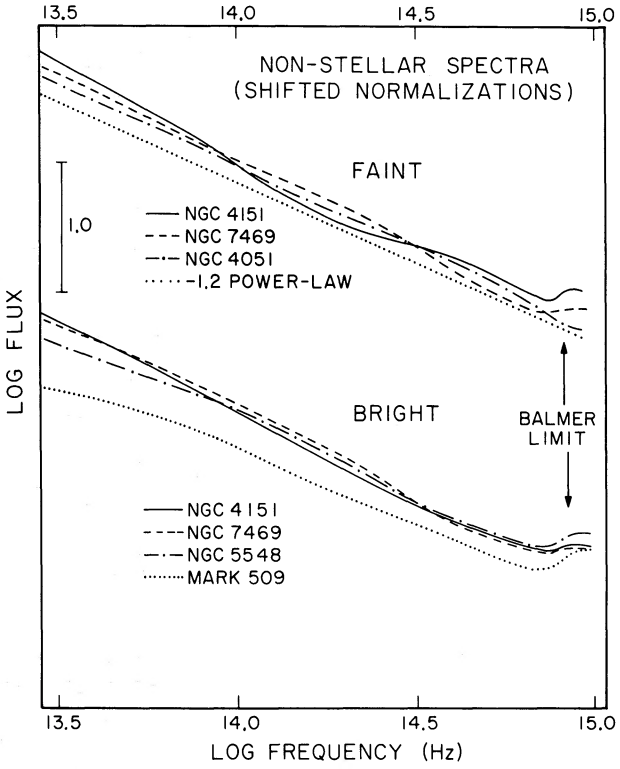

FIG. 9.—The nonstellar spectra from Fig. 8, rescaled for easy comparison with each other. The "faint" spectra fall steadily all the way to the Balmer limit and are not very different from the $f_\nu \propto \nu^{-1.2}$ power law shown for comparison. The "bright" nonstellar spectra are almost identical to that of Mrk 509, which has a detectable flattening in the blue well before the Balmer limit.

this curvature to continue to longer and shorter wavelengths. The 10–100 μm spectra of Seyfert 1 nuclei should show noticeable curvature and an overall slope which is flatter than -1.0. Note that on the scale of Figure 9, even a 10% error in the relative calibration of optical and infrared fluxes would still have no discernible effect on our results.

Our estimate of stellar flux in NGC 1068 is slightly higher than that obtained by Malkan and Oke (1983). Since it is based on better observations, it supersedes the previous value. The estimate of starlight flux in NGC 4151 is lower than that of Schmidt and Miller (1980), probably because they assumed the nonstellar light was a flat power law ($f_\nu \propto \nu^{-0.33}$).

Rieke (1978, 1981) has made estimates of the starlight flux in NGC 4151 and in several other low-luminosity Seyfert nuclei to examine their nonstellar infrared spectra. In NGC 4151, he assumed that the red spectrum at minimum light is entirely due to stars. Our spectra of the nucleus of NGC 4151 at minimum do not confirm this, since all of its absorption lines are far too weak to arise from pure undiluted starlight. Thus, Rieke's estimate of the stellar flux in 4151 is $\sim 50\%$ too high. Consequently, the nonstellar spectrum of NGC 4151 at minimum is not qualitatively different from that at maximum brightness: both fall smoothly from 2–3 μm to the visual, roughly with a power-law slope of -1.1 to -1.2. There is no short-wavelength break around 1 μm. If the bulk of the 2 μm flux comes from hot dust grains, as has been suggested by Rieke (1978) and reiterated by other investigators (Rieke and Lebofsky 1979; Angel and Stockman 1980), such a thermal Boltzmann cutoff in the nonstellar spectrum should be observable. Since it is not seen in any of our Seyfert 1 spectra, which instead have an approximately power-law shape (as in quasars), we conclude that *the bulk of their 2 μm flux is not thermal*.

Careful photometric monitoring by Lebofsky and Rieke (1980) shows that the blue and infrared variations in NGC 4151 and in the low-redshift quasar III Zwicky 2 are sometimes not instantaneously correlated. If (as MS argue) the blue light is predominantly thermal, while the red is nonthermal, they may not always vary synchronously. Rieke's measurements also show that the nonstellar infrared continuum may steepen slightly when it fades.

Although our results severely restrict the role that thermal dust emission could play in contributing to the near-infrared flux, they do not conclusively rule out the possibility that thermal emission may become important at longer wavelengths in many Seyfert 1 nuclei. For example, the "power law" seen at shorter wavelengths could turn over beyond 3 μm if the right amount of thermal emission from dust at $T \sim 500$ K were present to preserve the linearity of the resulting spectrum. Yet it seems implausible that the thermal and nonthermal fluxes would always be so well balanced: one should expect to see some spectra with a sharp (exponential) increase to longer wavelengths, as well as some with a turnover at 10 μm. This conflicts with the great uniformity of most infrared spectra of Seyfert 1 nuclei and quasars.

The starlight fluxes derived for NGC 1068 in the blue and red agree fairly well with those estimated by Malkan and Oke (1983). However, our high-quality near-infrared spectrum shows that the Ca II lines are probably seen at full strength in the nucleus of NGC 1068. At most, 10% of the near-infrared continuum within a 10″ aperture is nonstellar, indicating that the "power law" seen by Malkan and Oke (1983) at shorter wavelengths has flattened by 8000 Å. Since the nonstellar light is bluer than the starlight, the increase in polarization at shorter wavelengths is probably due to the nonstellar component (cf. Visvanathan and Oke 1968; Miller 1983). Our failure to detect dilution from nonstellar light at 8500 Å in NGC 1068 indicates that at least some Seyfert 2 galaxies do not have the same near-infrared power law that is generally present in type 1 Seyferts. It is not possible to ascertain whether the nonthermal component extends into the infrared in Seyfert 2 nuclei because this portion of their spectra is dominated by thermal emission from dust with a maximum temperature of 300–800 K (Malkan and Oke 1983). The same complication arises in the unusually red spectra of a few heavily reddened Seyfert 1 galaxies such as Mrk 231, which have very steep infrared spectra that are predominantly thermal (Rieke 1976).

VI. SUMMARY

Coudé spectroscopy and direct imaging have been combined to estimate the starlight fluxes in the nuclei of nine nearby Seyfert galaxies. The starlight colors agree with those expected in early-type spiral galaxies. The nonstellar continuum in low-luminosity Seyfert 1 nuclei is similar to that of very luminous Seyfert galaxies and quasars. It falls from the infrared to the visual roughly as a power law with a slope of -1.1 to -1.2. Except in the least luminous Seyfert nuclei studied, there is also a flattening before the Balmer limit, which has been attributed to optically thick thermal emission. Even at minimum brightness, there is no spectral steepening at wavelengths less than 1 μm, ruling out a thermal origin for the bulk of the 2 μm emission.

During the many nights required to obtain the data, expert assistance was provided by Howard Lanning and Jim Frazer at Mount Wilson, Skip Staples and Bob Griffith at Palomar, and Oscar Duhalde, Fernando Peralta, and Angel Guerra at Las Campanas. We are grateful to A. G. de Bruyn, A. C. S. Readhead, and W. L. W. Sargent for private communication of unpub-

lished data, as well as Abi Saha and James Fillmore for some of the computer programs used in the analysis. Informative discussions with J. B. Oke, G. H. Rieke, W. L. W. Sargent, and D. P. Schneider are appreciated, and we thank H. K. C. Yee for particularly illuminating conversations. This work was supported by the Fannie and John Hertz Foundation through two graduate fellowships, and by the National Science Foundation through grant AST-8216544 to W. L. W. Sargent.

APPENDIX

LINE PROFILES AND NEW EMISSION LINES

The data obtained for this investigation have also been used in a study of the emission lines in Seyfert galaxies. Although a detailed analysis will be presented elsewhere (Filippenko and Malkan 1983), a few conclusions are briefly discussed here.

Several new emission lines have been identified in the coudé spectra. One is He II λ8237, in NGC 4151 (Fig. 3). Careful examination of Figure 1 in Grandi (1978) reveals that the feature may also be present in NGC 1068, NGC 4051, and Mrk 335, but this must be confirmed with spectra of higher quality. In principle, He II λ8237 can be used together with He II λ4686 as a reddening indicator; the signal-to-noise ratio in our data, however, is not sufficiently large.

A stronger and more puzzling line in NGC 4151 is at $\lambda \sim 8617$ Å. It is narrow, and therefore probably corresponds to a forbidden transition. Several spectra obtained by J. B. Oke (1983) confirm the presence of this line. The most likely identification is [Fe II] λ8617, which is also visible in the Eta Carinae nebula (Thackeray 1953) and in the Orion nebula (Grandi 1975; Danziger and Aaronson 1974). A considerably broader feature appears at approximately the same wavelength in NGC 1068 (Fig. 3), but the width is consistent with that of other forbidden lines in this object.

Still another line which (to our knowledge) has not been previously reported in Seyfert galaxies appears at $\lambda \sim 5120$ Å in NGC 4051, 4151, 7469, and possibly 1068. Although its exact identification is unknown, it is probably a forbidden line from a highly ionized species, since [Fe VII] emission is strong in these galaxies. The feature also appears in NGC 6741 and IC 418 (Aller and Walker 1970), two planetary nebulae which exhibit lines from multiply ionized elements, but surprisingly it may be absent in other high-excitation planetary nebulae (Kaler 1976).

With high spectral resolution, we can investigate line profiles and small differences in the width and redshift of lines which represent a wide range of excitation. Such studies will provide information concerning the kinematics and geometry of the gas and dust in Seyfert nuclei. For example, the width of the [Fe VII]+[Ca V] λ6087 line in NGC 1068 and NGC 7469 is considerably greater than that of [O I] λ6300, and in Mrk 335 the widths differ by a factor of 2–3. A similar increase in line width with increasing ionization potential of the corresponding ion has been noticed in several other Seyfert galaxies (Osterbrock 1981; Pelat, Alloin, and Fosbury 1981) and indicates that the cloud velocity dispersion is greatest near the central source of ionizing radiation. Moreover, the difference between the redshift of emission and absorption lines in NGC 1068, which was first noticed by Burbidge, Burbidge, and Prendergast (1959), is confirmed, and slight discrepancies are evident in other objects as well.

A search for broad wings in the emission lines has also been conducted. For example, NGC 1068 may have a very faint, broad component of Hβ which qualitatively resembles that of Seyfert 1 galaxies. Similarly, the Hβ profile in NGC 5548 has three distinct components: one corresponds to the narrow forbidden lines, another has a width which is typical of that in type 1 Seyfert galaxies, whereas the third may extend redward of [O III] λ5007 and is reminiscent of the extremely broad wings seen in broad-line radio galaxies (Osterbrock, Koski, and Phillips 1976). Finally, it is possible that very weak wings are present in the [O III] λ4959, 5007 lines of NGC 4151, but this must be confirmed in future investigations.

REFERENCES

Aller, L. H., and Walker, M. F. 1970, *Ap. J.*, **161**, 917.
Alloin, D., Laques, P., Pelat, D., and Despiau, R. 1981, *Astr. Ap.*, **95**, 394.
Angel, J. R. P., and Stockman, H. S. 1980, *Ann. Rev. Astr. Ap.*, **18**, 321.
Balzano, V. A., and Weedman, D. W. 1981, *Ap. J.*, **243**, 756.
Burbidge, E. M., Burbidge, G. R., and Prendergast, K. H. 1959, *Ap. J.*, **130**, 26.
Cohen, J. G. 1978, *Ap. J.*, **221**, 788.
Cutri, R. M., *et al.* 1981, *Ap. J.*, **245**, 818.
Danziger, I. J., and Aaronson, M. 1974, *Pub. A.S.P.*, **86**, 208.
de Bruyn, A. G. 1982, private communication.
de Bruyn, A. G., and Sargent, W. L. W. 1978, *A.J.*, **83**, 1257.
de Bruyn, A. G., Sargent, W. L. W., and Readhead, A. C. S. 1982, private communication.
Filippenko, A. V. 1982, *Pub. A.S.P.*, **94**, 715.
Filippenko, A. V., and Malkan, M. A. 1983, in preparation.
Grandi, S. A. 1975, *Ap. J. (Letters)*, **199**, L43.
———. 1978, *Ap. J.*, **221**, 501.
Hartwick, F. J., and Cowley, A. 1980, *Ap. J.*, **235**, 755.
Kaler, J. B. 1976, *Ap. J. Suppl.*, **31**, 517.
Kent, S. M. 1979, *Pub. A.S.P.*, **91**, 394.

Kormendy, J., and Illingworth, G. 1982, *Ap. J.*, **256**, 460.
Lebofsky, M. J., and Rieke, G. H. 1980, *Nature*, **284**, 410.
Malkan, M. A. 1983*a*, *Ap. J. (Letters)*, **264**, L1.
_____. 1983*b*, *Ap. J.*, **268**, 582.
Malkan, M. A., Margon, B., and Chanan, G. 1983, *Ap. J.*, submitted.
Malkan, M. A., and Oke, J. B. 1983, *Ap. J.*, **265**, 92.
Malkan, M. A., and Sargent, W. L. W. 1982, *Ap. J.*, **254**, 22 (MS).
McAlary, C. W., McLaren, R. A., McGonegal, R. J., and Maza, J. 1983, *Ap. J. Suppl.*, **52**, 341.
McAlary, C. W., McLaren, R. A., and Crabtree, D. R. 1979, *Ap. J.*, **234**, 471.
Miller, J. S. 1983, preprint.
Minkowski, R. 1968, *A.J.*, **73**, 836.
Oke, J. B. 1969, *Pub. A.S.P.*, **81**, 11.
_____. 1983, private communication.
Oke, J. B., and Gunn, J. E. 1983, *Ap. J.*, **266**, 713.
Osterbrock, D. E. 1978, *Proc. Nat. Acad. Sci.*, **75**, 540.
_____. 1981, *Ap. J.*, **246**, 696.
_____. 1983, *Pub. A.S.P.*, **95**, 12.
Osterbrock, D. E., Koski, A. T., and Phillips, M. M. 1976, *Ap. J.*, **206**, 898.
Pelat, D., Alloin, D., and Fosbury, R. A. E. 1981, *M.N.R.A.S.*, **195**, 787.
Penston, M. V., *et al.* 1974, *M.N.R.A.S.*, **169**, 357.
Phillips, M. M. 1977, *Ap. J.*, **215**, 740.
_____. 1978, *Ap. J. Suppl.*, **38**, 187.
Rieke, G. H. 1976, *Ap. J. (Letters)*, **206**, L15.
_____. 1978, *Ap. J.*, **226**, 550.
_____. 1981, *Ap. J.*, **250**, 87.
Rieke, G. H., and Lebofsky, M. J. 1979, *Ann. Rev. Astr. Ap.*, **17**, 477.
Rudy, R. J., Jones, B., Levan, P. D., Smith, H. E., Willner, S. P., and Tokunaga, A. T. 1982, *Ap. J.*, **257**, 570.
Schmidt, G. D., and Miller, J. S. 1980, *Ap. J.*, **240**, 759.
Shectman, S., and Hiltner, W. A. 1976, *Pub. A.S.P.*, **88**, 960.
Stauffer, J. 1983, *Ap. J.*, **264**, 14.
Thackeray, A. D. 1953, *M.N.R.A.S.*, **113**, 211.
Thuan, T. X., and Gunn, J. E. 1976, *Pub. A.S.P.*, **88**, 543.
Visvanathan, N., and Oke, J. B. 1968, *Ap. J. (Letters)*, **152**, L165.
Wade, R. A., Hoessel, J. G., Elias, J. H., and Huchra, J. P. 1980, *Pub. A.S.P.*, **91**, 35.
Yee, H. K. C. 1983, *Ap. J.*, **272**, 473.
Yee, H. K. C., and Oke, J. B. 1978, *Ap. J.*, **226**, 753.

ALEXEI V. FILIPPENKO and MATTHEW A. MALKAN: Department of Astronomy, 105-24, California Institute of Technology, Pasadena, CA 91125